Journal of Elasticity **43:** 109–136, 1996.

The Cantilever Strip Plate under Torsion, Bending or Flexure at Infinity

R. DOUGLAS GREGORY, CHONGHUA GU and FREDERIC Y.M. WAN
Dept. of Mathematics, University of Manchester, Manchester M13 9PL, England
Dept. of Mathematics, University of California at Irvine, Irvine, CA 92717, U.S.A.

Received 26 January 1996

Abstract. A homogeneous, isotropic plate occupies the region $0 \leqslant x_1 \leqslant \infty, |x_2| \leqslant a, |x_3| \leqslant h$, where the ratio h/a is sufficiently small so that the classical theory of thin plate bending applies. The short end of the plate at $x_1 = 0$ is clamped while the long sides are free. This cantilever plate is now loaded at $x_1 = +\infty$ by an applied twisting moment, by a bending moment or by flexure. Despite the fundamental nature of these problems, and the long history of thin plate theory, no solutions are to be found in the existing literature that will determine (for instance) the important unknown resultants V_1, M_{11} at the clamped end $x_1 = 0$. The main reason for this is that this combination of boundary conditions leads to severe oscillating singularities of the field in the corners $(0, \pm a)$. The fact that such singularities must exist is widely known, but we present here for the first time a method of solution that takes these singularities fully into account.

Our numerical results show that the values of M_{11}, V_1 on $x_1 = 0$ bear little resemblance to those of the corresponding Saint-Venant 'solutions', which do not fully satisfy the boundary conditions at the clamped end. Indeed, significantly large values of these resultants were found at points far enough from the corners so as to be relevant in actual engineering applications. Also of interest are certain weighted integrals of M_{11}, V_1 which we calculate. These constants determine the effect of the clamping at 'large' distances (greater than $4a$, say) from the clamped end. At such distances, the effect of the clamping is merely to impose an additional rigid body deflection on the plate.

Finally, we consider the plate of finite length. Provided that the aspect ratio is 2 or more, we give accurate approximate solutions for the torsion, bending or flexure of a finite plate clamped at both ends.

1. Introduction

The classical theory of the bending of thin rectangular plates with various edge conditions is extremely well documented. Indeed, Timoshenko & Woinowsky–Kreiger [6] devote two entire chapters to the study of particular cases. However, almost all this work is restricted to cases in which the plate has *two opposite edges simply supported* and with various conditions at the other two edges. This restriction greatly simplifies the analysis, since the solution of the governing equation for the transverse deflection w can be analytically continued across such boundaries by anti-reflection. This means that the solution for the rectangle is identical to that for an infinite strip plate with periodic conditions on its two infinite edges. No such simplification is available for a 'cantilever' plate which has two opposite edges free and a third edge clamped (built-in). This is one reason why there is relatively little known about what is a fundamental engineering problem. A second reason is

the presence of severe singularities at the corner points where the free sides of the plate meet the clamped end. Since the work of Williams [7], it has been known how to find the exponents of such singularities, which depend only on the two boundary conditions, the corner angle and Poisson's ratio. The corner singularities in the present case are much worse than in the corresponding plane strain problems. In the plane strain case, the exponent is always real (when the material is homogeneous and isotropic) and is such that the tractions at the clamped end are $\mathcal{L}^2$-functions. However, in the case of the cantilever plate, the exponent is such that the shear resultants at the clamped end are almost non-integrable. Even worse, for most choices of Poisson's ratio, the exponent is *complex* so that the singularities are oscillating as well. For a method of solution to be successful, it is essential that the known form of the corner singularities be incorporated into it.

A well established method for treating such problems is the singular integral equation method of Erdogan, Gupta & Cooke [1]. In this method, the singularities are normalised out to create new regular unknowns, which are shown to satisfy singular integral equations; these equations can then be solved numerically. However, this method requires the singular exponent to be real, and any extension to the complex exponent case is far from obvious. The method used in the present work is an extension (and improvement upon) the *method of projection* introduced by Gregory & Gladwell [2], [3]. It is a method particularly suited to the case of the semi-infinite cantilever plate, which is the principal object of our investigation. Taking the plate to be semi-infinite is an important simplification which does not restrict applicability as much as might be imagined. A finite plate need not be very long in order to be effectively semi-infinite; as we will see, any aspect ratio greater than about 2 is enough.

Suppose then that the plate occupies the region $0 \leqslant x_1 < \infty, |x_2| \leqslant a, |x_3| \leqslant h$ as shown in Figure 1, where the sides $x_2 = \pm a$ are free and the end $x_1 = 0$ is clamped. We consider three basic problems in which the plate is loaded by being subject to torsion, bending or flexure applied at $x_1 = +\infty$. The principal unknown quantities of interest here are the effective shear resultant $V_1(0, x_2)$ and moment resultant $M_{11}(0, x_2)$ induced at the clamped end. In the method of projection, a reciprocity formula is used to show that the required vector function

$$\mathbf{u}(x_2) = \begin{pmatrix} V_1(0, x_2) \\ M_{11}(0, x_2) \end{pmatrix}, \tag{1.1}$$

considered as a member of the Hilbert space $\mathcal{H} = \mathcal{L}^2[-1, 1]$, is orthogonal to a certain subspace of $\mathcal{H}$. If the orthogonal complement of this subspace is one-dimensional, this provides a method for determining $\mathbf{u}$. In the improved method, we define new unknowns $\widehat{V}_1(x_2), \widehat{M}_{11}(x_2)$ by

$$V_1(0, x_2) = (1 - x_2^2)^{\alpha} \widehat{V}_1(x_2), \tag{1.2}$$

$$M_{11}(0, x_2) = (1 - x_2^2)^{1+\alpha} \widehat{M}_{11}(x_2), \tag{1.3}$$

where α is the *real part* of the complex exponent of the corner singularities of V_1, and we construct the new unknown vector $\widehat{\mathbf{u}}(x_2)$ by

$$\widehat{\mathbf{u}}(x_2) = \begin{pmatrix} \widehat{V}_1(x_2) \\ \widehat{M}_{11}(x_2) \end{pmatrix}. \tag{1.4}$$

The original reciprocity relations are now reinterpreted as orthogonality relations on $\widehat{\mathbf{u}}$, considered as a member of a new Hilbert space $\mathcal{H}_\alpha$. This procedure effectively removes the infinities in the corner singularities, the new unknown $\widehat{\mathbf{u}}$ having (infinitely many) oscillations of bounded amplitude near $x_2 = \pm a$. In Sections 3, 4, 5 we give a fuller description of this method including the quite subtle procedure for handling the remaining oscillatory singularities of $\widehat{\mathbf{u}}$. We are not aware of any other general method which is appropriate for the handling of this kind of oscillating singularity.

Our numerical results for all three problems are set out in Section 6. The method was very effective in that relatively small systems of equations gave values for $\widehat{\mathbf{u}}(x_2)$ correct to about 3 decimal places. The only direct comparison we could make with previous work was with the results of Koiter & Alblas [4], who gave a partial solution to the bending problem. Although these authors were aware of the nature of the corner singularities, their Fourier transform method did not incorporate this knowledge. As a result, they were not able to determine $V_1(0, x_2)$ at all, but they did find values for $M_{11}(0, x_2)$ (for the case in which $\nu = \frac{1}{4}$). Their results differ from ours by a few percent across the range, but we regard our results as the more accurate since they incorporate the corner behaviour correctly. In particular, Koiter & Alblas's value for $M_{11}(0, \pm a)$ is not zero, as is required from the boundary conditions. In general, our numerical results show that the values of M_{11}, V_1 on $x_1 = 0$ bear little resemblance to those of the corresponding Saint-Venant 'solutions', which do not fully satisfy the boundary conditions at the clamped end. Indeed, significantly large values of these resultants were found at points far enough from the corners so as to be relevant in actual engineering applications. We also calculate certain weighted integrals of $V_1(0, x_2), M_{11}(0, x_2)$ over the interval $[-a, a]$. These are important in that they determine the behavior of the solutions at 'large' distances from the clamped end. At such distances, the effect of the clamping is merely to impose an additional rigid body deflection on the plate. As might be expected, these integrated quantities are found more accurately than their corresponding integrands, typically to about 6 decimal places. These integrals also provide a valuable check on our entire solution process, since two of them can be shown to be linked by a reciprocity identity. This identity was not used anywhere in our calculations but was found to be satisfied correct to 6 decimal places.

Finally, in Section 7, we return to the plate of finite length. Provided that the aspect ratio is 2 or more, we give accurate approximate solutions for the torsion,

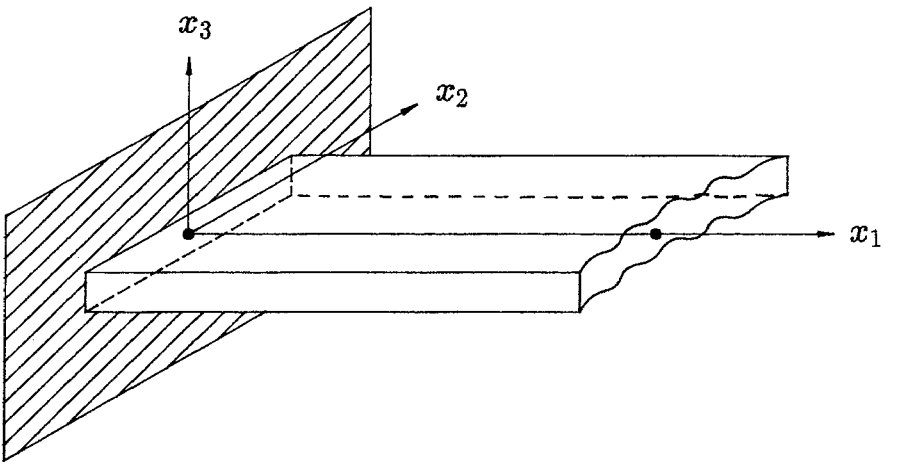

Figure 1. The semi-infinite cantilever plate under torsion $\mathcal{T}$, bending $\mathcal{M}$ or flexure $\mathcal{F}$ at infinity.

bending or flexure of a finite plate clamped at both ends. Our formulae for the response of the plate involve the weighted integrals calculated in Section 6.

2. Description of the Problems

The semi-infinite plate shown in Figure 1 occupies the region $0 \leqslant x_1 < \infty, |x_2| \leqslant a, |x_3| \leqslant h$. The plate is composed of homogeneous, isotropic, linearly elastic material with Young's modulus E and Poisson's ratio ν. We further suppose that the ratio h/a is sufficiently small so that the classical theory of bending of thin plates applies (see Appendix A). The end of the plate is clamped so that $w(x_1, x_2)$, the (small) transverse deflection of the mid-plane of the plate, satisfies

$$w(0, x_2) = 0, \tag{2.1}$$

$$w_{,1}(0, x_2) = 0 \tag{2.2}$$

($|x_2| \leqslant a$). However the sides of the plate are traction-free so that the Kirchhoff contracted boundary conditions hold, namely,

$$V_2(x_1, \pm a) = 0, \tag{2.3}$$

$$M_{22}(x_1, \pm a) = 0 \tag{2.4}$$

($0 < x_1 < \infty$), where V_2, M_{22} are the effective shear resultant and bending moment respectively (see Appendix A where (2.3), (2.4) are expressed in terms of w).

This 'cantilever' plate is now loaded at $x_1 = +\infty$ by one of the following force systems:

(i) torsion with prescribed twisting moment $\mathcal{T}$,
(ii) (pure) bending with prescribed bending moment $\mathcal{M}$,
(iii) flexure* with transverse load $\mathcal{F}$.

In terms of the moment resultants $\mathbf{M}(= (M_{\alpha\beta}), 1 \leqslant \alpha, \beta \leqslant 2)$ defined by (A.2), this requires that

$$\text{Torsion Problem}: \quad \mathbf{M} \to \frac{\mathcal{T}}{4a}\begin{pmatrix} 0 & -1 \\ -1 & 0 \end{pmatrix}, \tag{2.5}$$

$$\text{Bending Problem}: \quad \mathbf{M} \to \frac{\mathcal{M}}{2a}\begin{pmatrix} 1 & 0 \\ 0 & 0 \end{pmatrix}, \tag{2.6}$$

$$\text{Flexure Problem}: \quad \mathbf{M} = \frac{\mathcal{F}}{2a(1-\nu)}\begin{pmatrix} x_1 & -\nu x_2 \\ -\nu x_2 & 0 \end{pmatrix} + o(1) \tag{2.7}$$

as $x_1 \to +\infty$, uniformly for $|x_2| \leqslant a$.

Some restriction must also be placed on the behaviour of $w(x_1, x_2)$ near the corner points $(0, \pm a)$ in order to exclude 'unphysical' solutions. We require that the plate should have bounded strain energy near these corners. The precise nature of the corner singularities which *are* permitted is given in Appendix B; these singularities have a profound effect on the solution process.

The problem to be solved in each case is to determine the deflection (and the corresponding shear and moment resultants) in the plate, and especially to determine the unknown resultants $V_1(0, x_2)$, $M_{11}(0, x_2)$ at the clamped end $x_1 = 0$.

3. The Improved Method of Projection

To illustrate the solution procedure, we consider the torsion problem; special features of the bending and flexure problems will be noted later. Also, without losing generality, we take $a = 1$ so that the plate has width 2; the solution for the case of general width can be deduced by scaling.

We begin by applying the reciprocity formula (C.11) proved in Appendix C. The integration contour C is taken to be the indented rectangular contour $C_{\delta,X}$ shown in Figure 2. The #1-state is taken to be the solution to the torsion problem (for the plate of width 2), while the #2-state is taken to be any of the exponentially decaying (anti-symmetric) PF-eigenfunctions for the plate, obtained in Appendix D. These eigenfunctions have the form

$$w^{\lambda}(x_1, x_2) = F^{\lambda}(x_2)\, \mathrm{e}^{-\lambda x_1}, \tag{3.1}$$

* Here the term 'flexure' means a combination of transverse load and bending moments so that the applied bending moment at $x_1 = 0$ is zero

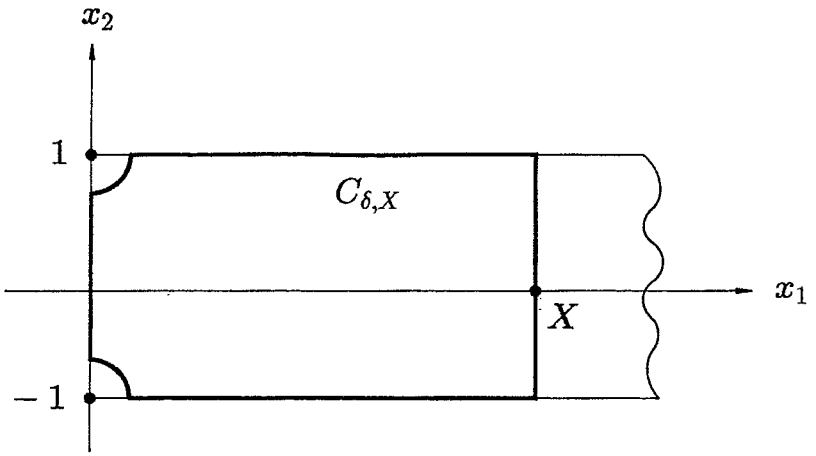

Figure 2. The contour $C_{\delta,X}$, a rectangle indented by quarter circles of radius δ at the corners $(0, \pm 1)$.

where the function $F^\lambda(x_2)$ is given explicitly by (D.7) and λ is any one of the countable infinity of roots of the secular equation (D.6) that have positive real part.

The contributions to the reciprocity formula form the arcs $\delta \leqslant x_1 \leqslant X, |x_2| = \pm 1$ are identically zero since both the chosen states satisfy the Kirchhoff boundary conditions (2.3), (2.4) there. The contribution from the arc $x_1 = X, |x_2| \leqslant 1$ tends to zero as $X \to \infty$, since the PF-eigenfunctions are exponentially small as $x_1 \to \infty$, while the torsion solution has (at worst) algebraic growth. The contributions from the quarter circles need more careful consideration since the torsion solution has singularities at the points $(0, \pm 1)$. However, for $\nu \geqslant 0$, the exponent of the singularities is such that these contributions do tend to zero* as $\delta \to 0$ (see Appendix B). Thus, on letting $X \to \infty$ and $\delta \to 0$, the reciprocity formula yields

$$\int_{-1}^{1} V_1 w^\lambda - M_{11} w^\lambda_{,1} |_{x_1=0} \, \mathrm{d}x_2 = \int_{-1}^{1} V_1^\lambda w - M_{11}^\lambda w_{,1} |_{x_1=0} \, \mathrm{d}x_2, \tag{3.2}$$

where $w^\lambda, M^\lambda_{\alpha\beta}, V^\lambda_\alpha$ belong to the PF-eigenfunction (3.1) while $w, M_{\alpha\beta}, V_\alpha$ belong to the solution to the torsion problem. On taking account of the boundary conditions (2.1), (2.2) satisfied by w, and the formula (3.1), this becomes

$$\int_{-1}^{1} \{V_1(0, x_2) F^\lambda(x_2) + M_{11}(0, x_2) \lambda F^\lambda(x_2)\} \, \mathrm{d}x_2 = 0. \tag{3.3}$$

Formula (3.3) is a set of identities satisfied by the important unknown resultants V_1, M_{11} at the clamped end $x_1 = 0$. Recall that $F^\lambda(x_2)$ is given by (D.7) while λ

* For $\nu < 0$ this is not true and the method of solution employed here fails. Fortunately, negative values of ν are not of great interest.

is any root of (D.6) with positive real part; this set of values of λ will be denoted by Λ.

Gregory & Gladwell [2], [3] have devised a method, called the *method of projection*, to determine the functions $V_1(0, x_2)$, $M_{11}(0, x_2)$ directly from a system of identities such as (3.3). They regarded such identities as a set of inner-product relations

$$\left\langle \begin{pmatrix} V_1 \\ M_{11} \end{pmatrix}, \begin{pmatrix} F^\lambda \\ \lambda F^\lambda \end{pmatrix} \right\rangle = 0 \tag{3.4}$$

($\lambda \in \Lambda$) between members of a Hilbert space $\mathcal{H}$ of vector functions lying in $\mathcal{L}^2[-1, 1]$. The unknown vector

$$\mathbf{u} = \begin{pmatrix} V_1 \\ M_{11} \end{pmatrix}$$

is then orthogonal to the linear subspace $\mathcal{D}(\subset \mathcal{H})$ spanned by $\binom{F^\lambda}{\lambda F^\lambda}$, $(\lambda \in \Lambda)$. If the orthogonal complement of $\bar{\mathcal{D}}$ (in $\mathcal{H}$) is one-dimensional, this provides a method of determining $\mathbf{u}$. Starting from any $\mathbf{h} \in \mathcal{H}$, first find $\mathbf{d}$, the projection of $\mathbf{h}$ onto $\bar{\mathcal{D}}$. Then $\mathbf{h} - \mathbf{d}$ must be a multiple of $\mathbf{u}$ and this multiple can be found by normalisation. Details of this procedure, including the approximate determination of $\mathbf{d}$, are given in [2].

Strictly speaking, the above procedure does not apply to the present problems. This is because both components of the unknown $\mathbf{u}$ are required to lie in $\mathcal{L}^2[-1, 1]$. For the problems treated by Gregory and Gladwell in [2], [3], this was true, but, in the present problems, the real part of the exponent of the corner singularities of $V_1(0, x_2)$ is less than $-\frac{1}{2}$, so that $V_1(0, x_2)$ does not lie in $\mathcal{L}^2[-1, 1]$ (see Appendix B). We therefore present below an improved version of the method of projection which overcomes this difficulty, and is superior generally. This improved method

(i) applies when $\mathbf{u}$ has *any* integrable singularities at $x_2 = \pm 1$,
(ii) converges to give accurate results much more rapidly than the original method, as the number of PF-eigenfunctions used is increased,
(iii) is able to handle the severe additional difficulty that the exponent of the corner singularities is actually *complex* (for most choices of ν).

The improved method of projection

From Appendix B, the Williams eigenfunctions for the corner at (0,1) have resultants on $x_1 = 0$ of the form

$$V_1(0, x_2) = K_1(1 - x_2)^{\alpha + i\beta}, \tag{3.5}$$

$$M_{11}(0, x_2) = K_2(1 - x_2)^{1 + \alpha + i\beta}, \tag{3.6}$$

($x_2 < 1$), where $\alpha, \beta, K_1/K_2$ depend only on ν (α, β are real, but K_1/K_2 is complex in general). Values of α, β for the *leading* Williams eigenfunction are given in Appendix B, Table 2 for $\nu = 1/4, 1/3, 1/2$. From now on we will always suppose that (3.5), (3.6) refer to this leading eigenfunction. In the torsion problem then, the *asymptotic* forms of $V_1(0, x_2), M_{11}(0, x_2)$ as $x_2 \to 1-$ must be some (complex) linear combinations of (3.5), (3.6) and their complex conjugates.

We define new unknowns* $\widehat{V}_1(x_2), \widehat{M}_{11}(x_2)$ by

$$V_1(0, x_2) = (1 - x_2^2)^{\alpha} \widehat{V}_1(x_2), \tag{3.7}$$

$$M_{11}(0, x_2) = (1 - x_2^2)^{1+\alpha} \widehat{M}_{11}(x_2), \tag{3.8}$$

in terms of which (3.3) can be written

$$\int_{-1}^{1} \left\{ \left(1 - x_2^2\right)^{\alpha} \widehat{V}_1(x_2) F^{\lambda}(x_2) + \left(1 - x_2^2\right)^{1+\alpha} \widehat{M}_{11}(x_2) \lambda F^{\lambda}(x_2) \right\} \mathrm{d}x_2 = 0, \tag{3.9}$$

for $\lambda \in \Lambda$.

We will still regard the identities (3.9) as orthogonality relations, but with respect to a new inner-product. Let $\mathbf{p}(x_2), \mathbf{q}(x_2)$ be complex valued two-component vector functions defined almost everywhere and odd on $[-1, 1]$. Define the inner-product

$$\langle \mathbf{p}, \mathbf{q} \rangle_{\alpha} = \int_{-1}^{1} \{(1 - x_2^2)^{\alpha} p_1 \bar{q}_1 + (1 - x_2^2)^{1+\alpha} p_2 \bar{q}_2\} \, \mathrm{d}x_2 \tag{3.10}$$

with associated norm

$$\|\mathbf{p}\|_{\alpha} = \{\langle \mathbf{p}, \mathbf{p} \rangle_{\alpha}\}^{1/2}. \tag{3.11}$$

Then

$$\mathcal{H}_{\alpha} \equiv \{\mathbf{p} : \|\mathbf{p}\|_{\alpha} < \infty\} \tag{3.12}$$

* When $\beta = 0$ (which is true only for very small values of ν), the transformation (3.7), (3.8) removes the leading term of the corner singularities so that $\widehat{V}_1, \widehat{M}_{11}$ are at least $C[-1, 1]$. This greatly simplifies their subsequent determination. For all 'practical' values of ν however, $\beta > 0$ and so $\widehat{V}_1, \widehat{M}_{11}$ still contain part of the corner singularity. They are no longer unbounded, but behave like linear combinations of

$$\left.\begin{matrix} \cos \\ \sin \end{matrix}\right\} [\beta \ln (1 - x_2^2)]$$

as $x_2 \to \pm 1$, and so have *infinitely many oscillations* of non-vanishing amplitude near $x_2 = \pm 1$. We will restrict our attention to this more important (and more difficult) case.

is a Hilbert space under the inner-product (3.10). Since $\alpha > -1$ in our application (see Table 2), it follows that

$$\hat{\mathbf{u}} = \begin{pmatrix} \widehat{V}_1 \\ \widehat{M}_{11} \end{pmatrix} \in \mathcal{H}_\alpha, \tag{3.13}$$

and

$$\begin{pmatrix} F^\lambda \\ \lambda F^\lambda \end{pmatrix} \in \mathcal{H}_\alpha, \tag{3.14}$$

for $\lambda \in \Lambda$.

The theory developed in [2], Sections 3, 4, now applies to the torsion problem provided that we replace the ordinary inner-product by (3.10). In particular, a sequence of approximations convergent to the (new) unknown $\hat{\mathbf{u}}$ can be constructed as follows:

Let $\{\lambda_n\}(n \geqslant 1)$ be the roots of the PF-eigenvalue equation (D.6) lying in the first quadrant and ordered by increasing real part*, and let

$$\mathbf{F}_n = \begin{pmatrix} F^{\lambda_n} \\ \lambda_n F^{\lambda_n} \end{pmatrix}. \tag{3.15}$$

Take *any* (real) element $\mathbf{h} \in \mathcal{H}_\alpha$ and choose the real coefficients $A_1, \ldots A_N, B_1, \ldots B_N$ so as to minimise

$$\left\| \mathbf{h} - \sum_{n=1}^{N} [A_n \Re\{\mathbf{F}_n\} + B_n \Im\{\mathbf{F}_n\}] \right\|_\alpha \tag{3.16}$$

for each fixed N. Then, as $N \to \infty$,

$$\mathbf{h} - \sum_{n=1}^{N} [A_n \Re\{\mathbf{F}_n\} + B_n \Im\{\mathbf{F}_n\}] \to k\hat{\mathbf{u}}, \tag{3.17}$$

where $\hat{\mathbf{u}}$ is the required vector (3.13), k is an unknown constant and the convergence is in the sense of the $\mathcal{H}_\alpha$-norm. Formula (3.17) thus yields an 'un-normalised' $\hat{\mathbf{u}}$, but a simple normalisation can be performed (for $k \neq 0$) since, from overall equilibrium, $\hat{\mathbf{u}}$ is known to satisfy

$$\left\langle \hat{\mathbf{u}}, \begin{pmatrix} x_2 \\ 0 \end{pmatrix} \right\rangle_\alpha = \mathcal{T}, \tag{3.18}$$

* We present the theory for the case in which none of the λ_n is real, which is true (for instantance) when $\nu = \frac{1}{4}$. However, other values of ν may make λ_1, λ_2 real. In this case the associated eigenfunctions are also real and the terms in (3.16) containing their imaginary parts must be deleted.

where $\mathcal{T}$ is the applied twisting moment.

4. The Numerical Procedure

The expression (3.16) will be minimised if the coefficients $A_1, \ldots, A_N, B_1, \ldots, B_N$ satisfy the $2N \times 2N$ system of real simultaneous linear equations

$$\begin{pmatrix} \mathbf{W} & \mathbf{X} \\ \mathbf{Y} & \mathbf{Z} \end{pmatrix} \begin{pmatrix} \mathbf{A} \\ \mathbf{B} \end{pmatrix} = \begin{pmatrix} \mathbf{C} \\ \mathbf{D} \end{pmatrix}, \tag{4.1}$$

where $\mathbf{A} = (A_n), \mathbf{B} = (B_n)$, the $N \times N$ sub-matrices are given by

$$\mathbf{W} = (\langle \mathfrak{R}(\mathbf{F}_m), \mathfrak{R}(\mathbf{F}_n) \rangle_\alpha), \tag{4.2}$$

$$\mathbf{X} = (\langle \mathfrak{R}(\mathbf{F}_m), \mathfrak{F}(\mathbf{F}_n) \rangle_\alpha), \tag{4.3}$$

$$\mathbf{Y} = (\langle \mathfrak{F}(\mathbf{F}_m), \mathfrak{R}(\mathbf{F}_n) \rangle_\alpha), \tag{4.4}$$

$$\mathbf{Z} = (\langle \mathfrak{F}(\mathbf{F}_m), \mathfrak{F}(\mathbf{F}_n) \rangle_\alpha), \tag{4.5}$$

and the right hand side vector is given by

$$\mathbf{C} = (\langle \mathbf{h}, \mathfrak{R}(\mathbf{F}_m) \rangle_\alpha), \tag{4.6}$$

$$\mathbf{D} = (\langle \mathbf{h}, \mathfrak{F}(\mathbf{F}_m) \rangle_\alpha). \tag{4.7}$$

The system (4.1) is non-singular and its unique solution for $\mathbf{A}, \mathbf{B}$ may be substituted into the left side of (3.17) to yield an (un-normalised) approximation to $\hat{\mathbf{u}}$.

For any choice of the element $\mathbf{h}$, this approximation is known to converge (in the $\mathcal{H}_\alpha$-norm) to $k\hat{\mathbf{u}}$ as $N \to \infty$. However, for most choices of $\mathbf{h}$, this convergence would be slow. Suppose, for example, that $\mathbf{h}$ were taken to be a smooth function on $[-1, 1]$, say,

$$\mathbf{h}^{\text{reg}} = \begin{pmatrix} x_2 \\ 0 \end{pmatrix}. \tag{4.8}$$

The left side of (3.17) would then be smooth on $[-1, 1]$ for all N whereas $\hat{\mathbf{u}}$ is known to have oscillating singularities at $x_2 = \pm 1$ (see footnote on page 116). Thus the approximation (3.17) must have large pointwise errors near $x_2 = \pm 1$ for *any* N, and we find numerically that this is accompanied by very slow pointwise convergence over the rest of the interval.

This suggests that one should choose an $\mathbf{h}$ that mimics the actual behaviour of $\hat{\mathbf{u}}$ near $x_2 = \pm 1$. Consider the singular complex vector $\mathbf{h}^{\text{sing}}$ given by*

$$\mathbf{h}^{\text{sing}} = \begin{pmatrix} 2\frac{K_1}{K_2} x_2 (1 - x_2^2)^{i\beta} \\ x_2 (1 - x_2^2)^{i\beta} \end{pmatrix}, \tag{4.9}$$

where $K_1/K_2, \beta$, which depend only on ν, are defined in Appendix B. Since $\mathbf{h}^{\text{sing}}$ embodies the form of leading Williams eigenfunction present in $\hat{\mathbf{u}}$ at the corners $x_2 = \pm 1$, there exist unique constants a^*, b^* such that

$$\hat{\mathbf{u}} = a^* \mathfrak{R}(\mathbf{h}^{\text{sing}}) + b^* \mathfrak{F}(\mathbf{h}^{\text{sing}}) + \text{ function continuous on } [-1, 1]. \tag{4.10}$$

Interestingly though, *no* choice of $\mathbf{h}$ of the form

$$\mathbf{h} = a\mathfrak{R}(\mathbf{h}^{\text{sing}}) + b\mathfrak{F}(\mathbf{h}^{\text{sing}}) \tag{4.11}$$

will lead to rapid convergence of (3.17) as $N \to \infty$. The reason is that, although

$$\hat{\mathbf{u}} - a^* \mathfrak{R}(\mathbf{h}^{\text{sing}}) - b^* \mathfrak{F}(\mathbf{h}^{\text{sing}})$$

is continuous on $[-1, 1]$, it does not lie in $\bar{\mathcal{D}}$, where $\mathcal{D}$ is the linear space spanned by $\{\mathfrak{R}(\mathbf{F}_n), \mathfrak{F}(\mathbf{F}_n)\}$. To achieve rapid convergence of (3.17) as $N \to \infty$, it is necessary to select $\mathbf{h}$ from a more general class of the form

$$\mathbf{h} = a\mathfrak{R}(\mathbf{h}^{\text{sing}}) + b\mathfrak{F}(\mathbf{h}^{\text{sing}}) + c\mathbf{h}^{\text{reg}}, \tag{4.12}$$

where $\mathbf{h}^{\text{reg}}$ is any smooth function, for example (4.8). Then there exist unique constants a^*, b^*, c^* such that

$$\hat{\mathbf{u}} - \mathbf{h} \quad \text{is continuous on } [-1, 1], \tag{4.13}$$

$$\langle \hat{\mathbf{u}}, \hat{\mathbf{u}} - \mathbf{h} \rangle_\alpha = 0. \tag{4.14}$$

This is achieved by taking a, b as in (4.10) and then taking c to satisfy

$$\langle \hat{\mathbf{u}}, \hat{\mathbf{u}} \rangle_\alpha = a^* \langle \mathfrak{R}(\mathbf{h}^{\text{sing}}), \hat{\mathbf{u}} \rangle_\alpha + b^* \langle \mathfrak{F}(\mathbf{h}^{\text{sing}}), \hat{\mathbf{u}} \rangle_\alpha + c \langle \mathbf{h}^{\text{reg}}, \hat{\mathbf{u}} \rangle_\alpha. \tag{4.15}$$

(This is certainly possible with $\mathbf{h}^{\text{reg}}$ given by (4.8), for then $\langle \mathbf{h}^{\text{reg}}, \hat{\mathbf{u}} \rangle_\alpha = \mathcal{T} \neq 0$.) Thus there is a unique choice of the constants a, b, c in (4.12) giving an $\mathbf{h}$ which leads to rapid convergence of (3.17) as $N \to \infty$.

* The factor 2 in the upper component of $\mathbf{h}^{\text{sing}}$ compensates for the fact that the actual behaviour of V_1, M_{11} near $x_2 = 1$ involves $(1 - x_2)^\alpha, (1 - x_2)^{1+\alpha}$, whereas, in the inner-product (3.10), we use $(1 - x_2^2)^\alpha, (1 - x_2^2)^{1+\alpha}$.

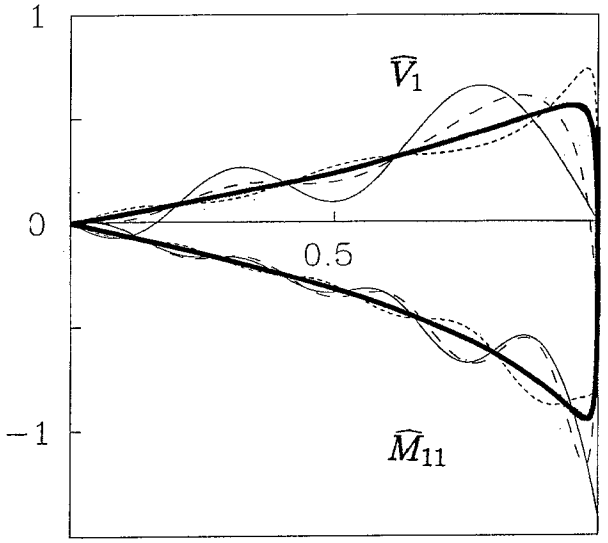

Figure 3. Values of $\widehat{V}_1, \widehat{M}_{11}$ against x_2 for the torsion problem, obtained by using different choices for $\mathbf{h}$; in all cases $\nu = \frac{1}{4}, a = 1, \mathcal{T} = 1$ and $N = 6$. The choices for $\mathbf{h}$ were (i) $\mathbf{h} = \mathfrak{R}(\mathbf{h}^{\text{sing}})$: – – –; (ii) $\mathbf{h} = \mathfrak{F}(\mathbf{h}^{\text{sing}})$: - - - - - - - -; (iii) $\mathbf{h} = \mathbf{h}^{\text{reg}}$: ————; (iv) $\mathbf{h}$ = optimum combination of (i), (ii), (iii): ▬▬▬.

The correct constants to take in (4.12) are not known beforehand and must be determined approximately as part of the solution process. The normalisation (3.18) gives one relation between the constants, but two more are needed. These can be provided as follows:

If $\mathbf{d}$ were the *exact* projection of the correct $\mathbf{h}$ (of the form (4.12)) onto $\bar{D}$, then the corner behaviour of $\hat{\mathbf{u}}$ requires that*

$$c\mathbf{h}^{\text{reg}}(1) - \mathbf{d}(1) = \mathbf{0}. \tag{4.16}$$

Our additional conditions on a, b, c are obtained by imposing the (vector) condition (4.16) on our *approximate* solution; that is, we require that a, b, c in (4.12) be such that

$$c\mathbf{h}^{\text{reg}}(1) - \sum_{n=1}^{N} [A_n \mathfrak{R}(\mathbf{F}_n(1)) + B_n \mathfrak{F}(\mathbf{F}_n(1))] = \mathbf{0} \tag{4.17}$$

for each N.

The remarkable improvement in convergence, obtained by taking $\mathbf{h}$ to be the 'optimum' linear combination of the form (4.12) is shown in Figure 3. With $N = 6$, the values of $\widehat{V}_1, \widehat{M}_{11}$, obtained by using (i) $\mathbf{h} = \mathfrak{R}(\mathbf{h}^{\text{sing}})$, (ii) $\mathbf{h} = \mathfrak{F}(\mathbf{h}^{\text{sing}})$, (iii)

* This is merely a statement that the second Williams eigenfunction for the corner at (0,1) is of order $o(1)$ as $x_2 \to 1$ compared to the leading eigenfunction.

$\mathbf{h} = \mathbf{h}^{\text{reg}}$ individually, all have large oscillations, different in each case. These oscillations are not present in the solution (iv) obtained by taking $\mathbf{h}$ as the optimum linear combination of (i), (ii), (iii). As N is increased, the *number* of oscillations in the solutions from choices (i), (ii), (iii) increases, while their *amplitude* slowly decreases. The solution from choice (iv) remains virtually unchanged as N is increased. Even when $N = 80$, the solutions from choices (i), (ii), (iii) are not as accurate as the solution from choice (iv) with $N = 6$.

Further Details of the Numerical Techniques

(i) Determination of the matrix elements (4.2)–(4.5) requires the numerical evaluation of integrals of the form*

$$\int_{-1}^{1} p(x_2)(1 - x_2^2)^{\alpha} \, \mathrm{d}x_2, \tag{4.18}$$

where $p(x_2) \in C^{\infty}[-1, 1]$. Such integrals can be quickly and accurately evaluated by Gauss-Jacobi quadrature. The necessary weights and abscissae (which depend upon α) were obtained by the NAG routine D01BCF [5]. In order to determine how many integration points were needed, some of these integrals were also evaluated (more expensively) by using the ordinary NAG integration routine D01AKF. (In this case the effect of the singularities at the end points was reduced by first making the substitution $x_2 = \sin \theta$.) We found that 200 integration points were sufficient to determine the matrix elements to at least 10 decimal digits. Similar remarks apply to the determination of the elements of $\mathbf{C}$, $\mathbf{D}$ when $\mathbf{h} = \mathbf{h}^{\text{reg}}$.

(ii) When $\mathbf{h} = \Re(\mathbf{h}^{\text{sing}}), \Im(\mathbf{h}^{\text{sing}})$, care must be exercised when evaluating the elements of $\mathbf{C}$, $\mathbf{D}$ because of the oscillating singularities these functions have at $x_2 = \pm 1$. Indeed, we found that a naïve application of Gauss-Jacobi quadrature (with 200 integration points) to integrands of this type gave answers that were completely wrong. For these integrands, we first make the substitution $x_2 = \tanh u$ so that (4.18) becomes

$$\int_{-\infty}^{\infty} \frac{p(\tanh u)}{(\cosh u)^{2+2\alpha}} \, \mathrm{d}u, \tag{4.19}$$

where $p(\tanh u)$ behaves like a linear combination of

$$\left.\begin{matrix}\cos \\ \sin\end{matrix}\right\} 2\beta|u| \tag{4.20}$$

as $|u| \to \infty$. The integral (4.19) can now be evaluated by using D01AKF over a truncated range $[-U, U]$ and then adding in *analytic* estimates of the contributions

* And also with α replaced by $1 + \alpha$.

from the 'tails'. In this way the integrals involving $\mathbf{h}^{\text{sing}}$ can be determined as accurately as those for $\mathbf{h}^{\text{reg}}$.

(iii) The linear system (4.1) was solved using LINPACK routines. The systems we used were not very large (never more than $N = 40$, even for checking) but we always checked the matrix condition number both for the system (4.1) and for an equivalent pre-scaled system which we used as a further check. We concluded that rounding error had no significant effect on our results.

5. The Bending and Flexure Problems

Since the bending and flexure problems are symmetrical about $x_2 = 0$, we now define the Hilbert space $\mathcal{H}_\alpha$ to consist of *even* functions on $[-1, 1]$ with the same inner-product (3.10). The elements $\{\mathbf{F}_n\}$ are replaced by their even counterparts $\{\mathbf{E}_n\}$, where

$$\mathbf{E}_n = \begin{pmatrix} E^{\lambda_n} \\ \lambda_n E^{\lambda_n} \end{pmatrix}. \tag{5.1}$$

In (5.1), $\{\lambda_n\}$ are the roots of the secular equation (D.3) lying in the first quadrant and the function $E^\lambda(x_2)$ is defined by (D.4). The orthogonal complement of the space spanned by $\{\mathfrak{R}(\mathbf{E}_n), \mathfrak{F}(\mathbf{E}_n)\}$ is *two-dimensional* and contains both the bending and flexure solutions. Thus, in addition to normalisation, we need an extra orthogonality condition to distinguish the two solutions, as follows:

Bending

$$\left\langle \hat{\mathbf{u}}, \begin{pmatrix} 1 \\ 0 \end{pmatrix} \right\rangle_\alpha = 0, \tag{5.2}$$

$$\left\langle \hat{\mathbf{u}}, \begin{pmatrix} 0 \\ 1 \end{pmatrix} \right\rangle_\alpha = \mathcal{M}. \tag{5.3}$$

Flexure

$$\left\langle \hat{\mathbf{u}}, \begin{pmatrix} 0 \\ 1 \end{pmatrix} \right\rangle_\alpha = 0, \tag{5.4}$$

$$\left\langle \hat{\mathbf{u}}, \begin{pmatrix} 1 \\ 0 \end{pmatrix} \right\rangle_\alpha = \mathcal{F}. \tag{5.5}$$

The additional orthogonality condition (5.2) (or (5.4)) must be incorporated into the linear system (4.1) which then has size $(2N + 1) \times (2N + 1)$.

The rest of the procedure closely follows that in the torsion case.

6. Results

As a check on the improved method of projection, we re-calculated the plane strain tension problem solved in [2]. In this problem, the exponent of the corner singularities is always real (that is, $\beta = 0$) so that the unknown $\hat{\mathbf{u}}$ has no oscillating singularities at $x_2 = \pm 1$ and can be found simply from a single smooth choice of $\mathbf{h}$. We obtained the same results as in [2] but were able to use *much smaller matrices*. Similar accuracy was obtained with $N = 10$ as was previously obtained with $N = 40$.

For the problems of the present paper, the exponent of the corner singularities is complex (except for very small values of ν). These problems were solved by the method described in Sections 3, 4, 5 which yields numerical values of $\widehat{V}_1(x_2), \widehat{M}_{11}(x_2)$. The physical quantities $V_1(0, x_2), M_{11}(0, x_2)$ can then be found from (3.7), (3.8). Note that, because of the boundary condition (2.2), the moment resultant $M_{12}(0, x_2) \equiv 0$, so that (see (A.9)) the shear resultant Q_1 and effective shear resultant V_1 are equal on $x_1 = 0$.

In Figures 4–9, we display these calculated values of (non-dimensionalised) $\widehat{V}_1(x_2)$ and $M_{11}(0, x_2)$. (We prefer to show graphs of $\widehat{V}_1$ rather than V_1 because V_1 is unbounded near $x_2 = \pm a$.) All of the graphs displayed in Figures 4–9 were calculated using $N = 20$. As a check, we recalculated these values using $N = 40$. This indicated that our calculated values for $\widehat{V}_1(x_2), \widehat{M}_{11}(x_2)$ were correct to about 3 decimal places, and there was no visible difference between the graphs for $N = 40$ and $N = 20$. Although our graphs in Figures 5, 7, 9, do not convey this impression, it is actually true that $M_{11}(0, a) = 0$ in each case. Like wise the (infinitely many) undamped oscillations of $\widehat{V}_1(x_2)$ near $x_2 = a$ are also invisible in Figures 4, 6, 8.

Care should be exercised before attributing direct physical significance to the values of $V_1(0, x_2), M_{11}(0, x_2)$ near $x_2 = \pm a$. The entire solution given here is in the context of the classical theory of thin plates, which is an approximate representation of three-dimensional elasticity, valid when h/a is small. In particular, it cannot be expected to represent the three-dimensional theory in regions lying within a distance of order $O(h)$ from a corner. This is not to say that the corner singularities of classical plate theory should be disregarded. They are a feature of that theory and an obstacle to finding the solution *anywhere*, not just near a corner. But in a more complete theory, the classical solution would be supplemented by 'corner boundary layers' with respect to which the classical theory would be the 'outer' solution. Thus the predictions of the classical theory should not be applied directly within these corner regions.

Torsion Problem – Figures 4, 5

As explained above, one should not attribute direct physical significance to the values taken by the solutions when $a - |x_2|$ is of order $O(h)$. However, the large

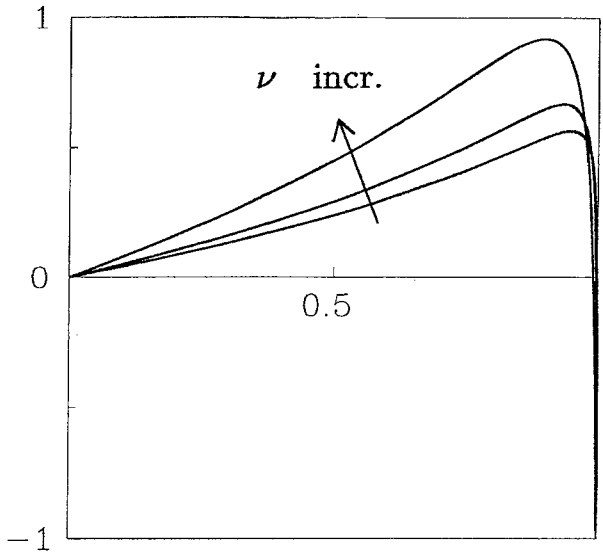

Figure 4. Torsion problem: Values of $a^2\mathcal{T}^{-1}\widehat{V}_1(x_2)$ against x_2/a for $\nu = 1/4, 1/3, 1/2$.

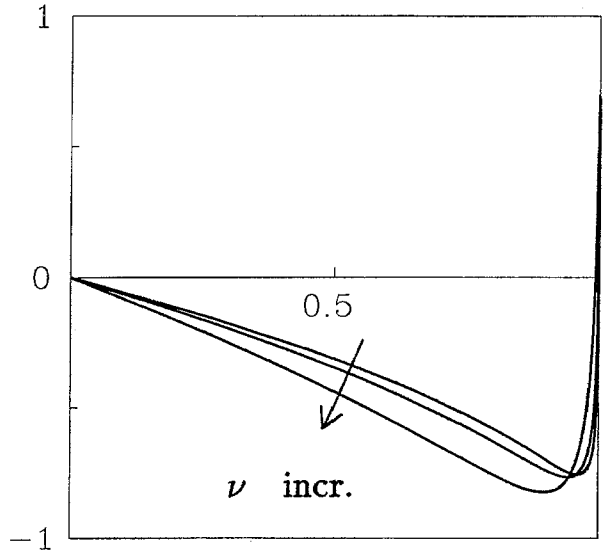

Figure 5. Torsion problem: Values of $a\mathcal{T}^{-1}M_{11}(0, x_2)$ against x_2/a for $\nu = 1/4, 1/3, 1/2$.

values achieved by $\widehat{V}_1(x_2)$ and $M_{11}(0, x_2)$ near $x_2 = \pm a$ may well lie outside these regions, and therefore actually occur; this merely requires that h/a should have a small but still realistic value ($h/a < 1/50$, say). For example, when $\nu = 0.5, a^2\mathcal{T}^{-1}V_1(0, 0.9a) \approx 4.55$, an unexpectedly large value; similar remarks apply to the values of $M_{11}(0, x_2)$ near $x_2 = \pm a$.

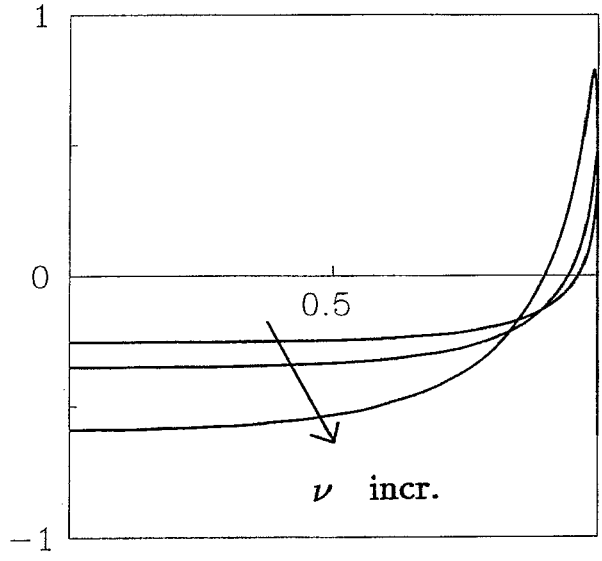

Figure 6. Bending problem: Values of $a^2\mathcal{M}^{-1}\widehat{V}_1(x_2)$ against x_2/a for $\nu = 1/4, 1/3, 1/2$.

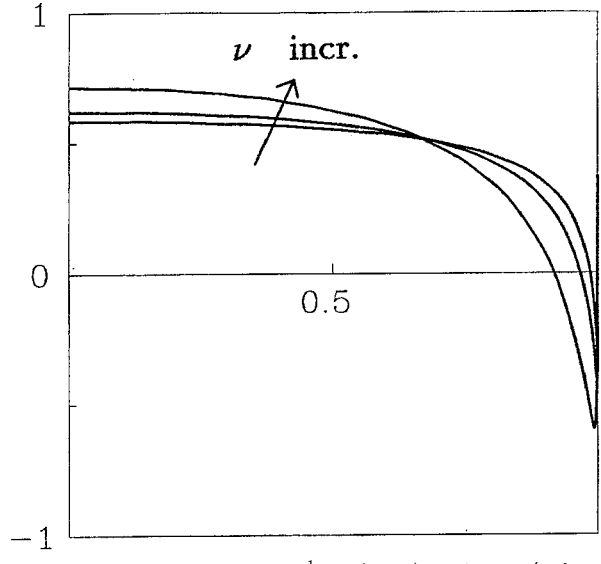

Figure 7. Bending problem: Values of $a\mathcal{M}^{-1}M_{11}(0, x_2)$ against x_2/a for $\nu = 1/4, 1/3, 1/2$.

Bending Problem – Figures 6, 7

In the bending problem, the large values of $\widehat{V}_1(x_2)$, $M_{11}(0, x_2)$ near $x_2 = a$ are achieved at points which are probably too close to $x_2 = a$ to be physically significant. However, the value of $a\mathcal{M}^{-1}M_{11}(0, 0)$ is siginificantly higher than the aver-

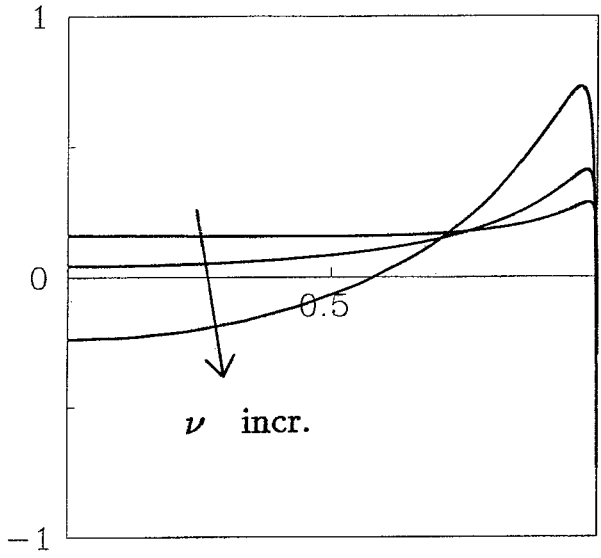

Figure 8. Flexure problem: Values of $a\mathcal{F}^{-1}\widehat{V}_1(x_2)$ against x_2/a for $\nu = 1/4, 1/3, 1/2$.

age value of $\frac{1}{2}$ predicted by the Saint-Venant bending 'solution'.* When $\nu = 1/2$, the value of $M_{11}(0,0)$ exceeds the Saint-Venant value by 43%, the corresponding figure for $\nu = 1/4$ being 17%. The cantilever plate bending problem has also been investigated by Koiter & Alblas [4]. Although these authors were aware of the nature of the corner singularities, they were not able to incorporate these singularities into their solution, as is the case with the method employed in the present paper. As a result, they were not able to calculate $V_1(0, x_2)$ at all, and their values for $M_{11}(0, x_2)$ are less accurate than ours. For instance, with $\nu = 1/4$, their value for $2a\mathcal{M}^{-1}M_{11}(0, a)$ is 0.066 instead of the exact value of zero required by the boundary conditions. Their value for $2a\mathcal{M}^{-1}M_{11}(0,0)$ is stated to be 1.208 ± 0.001, but our results, which do take the corner behaviour fully into account, indicate that this figure should be 1.169 ± 0.002.

Flexure Problem – Figures 8, 9

A remarkable feature of the flexure case is the behaviour of $V_1(0, x_2)$, (or equivalently $Q_1(0, x_2)$) for the larger values of ν. In the Saint-Venant flexure 'solution',** V_1 takes the constant value

$$V_1 = \frac{(1-\nu)\mathcal{F}}{2a(1+\nu)} \tag{6.1}$$

* The Saint-Venant bending solution does not satisfy the boundary condition (2.1) at $x_1 = 0$ (except when $\nu = 0$) and so is not actually the solution to our bending problem.

** The Saint-Venant flexure solution does not satisfy the boundary condition (2.2) at $x_1 = 0$ (except when $\nu = 0$) and so is not actually the solution to our flexure problem.

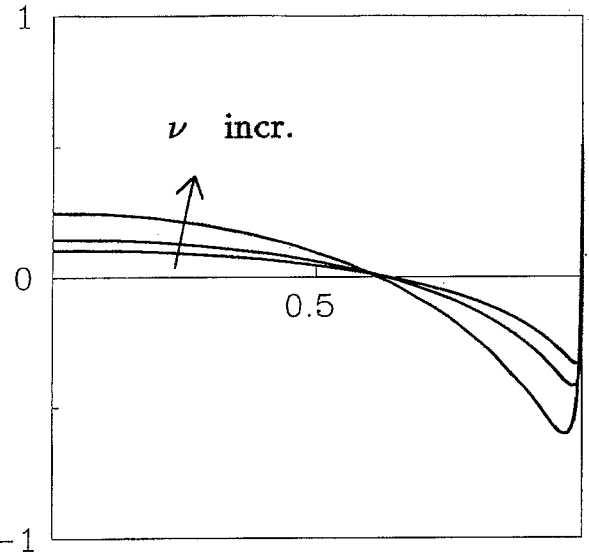

Figure 9. Flexure problem: Values of $\mathcal{F}^{-1}M_{11}(0, x_2)$ against x_2/a for $\nu = 1/4, 1/3, 1/2$.

on $x_1 = 0$, which, together with the edge values of M_{12}, balance the applied load. We see from Figure 8 however that, when $\nu = 1/2$, the actual values of V_1 have the 'wrong' sign over most of the interval; this is counterbalanced by large positive values near the ends of the interval. The value of $a\mathcal{F}^{-1}V_1(0, 0.95a) \approx 6.57$, which is over 39 times the Saint-Venant value $V_1 = \frac{1}{6}$ obtained from (6.1). This very large value of V_1 at $x_2 = 0.95a$ could certainly be physically significant for realistically small values of h/a.

Weighted Integrals of $V_1(0, x_2)$, $M_{11}(0, x_2)$

Of particular importance are certain weighted integrals of $V_1(0, x_2)$, $M_{11}(0, x_2)$. These integrals determine the behaviour of the solutions at 'large' distances from the clamped end. They are defined by

$$v_j^T = a^{1-j}\mathcal{T}^{-1}\int_{-a}^{a} x_2^j V_1^T(0, x_2)\,\mathrm{d}x_2, \tag{6.2}$$

$$m_j^T = a^{-j}\mathcal{T}^{-1}\int_{-a}^{a} x_2^j M_{11}^T(0, x_2)\,\mathrm{d}x_2, \tag{6.3}$$

$$v_j^B = a^{1-j}\mathcal{M}^{-1}\int_{-a}^{a} x_2^j V_1^B(0, x_2)\,\mathrm{d}x_2, \tag{6.4}$$

$$m_j^B = a^{-j}\mathcal{M}^{-1}\int_{-a}^{a} x_2^j M_{11}^B(0, x_2)\,\mathrm{d}x_2, \tag{6.5}$$

Table I. Values of the constants $m_1^T, v_2^B, m_2^B, v_2^F, m_2^F$ correct to 4 decimal places for $\nu = 1/4, 1/3, 1/2$

	$\nu = 1/4$	$\nu = 1/3$	$\nu = 1/2$
m_1^T	−0.4683	−0.4948	−0.5580
v_2^B	0.4128	0.5434	0.8071
m_2^B	0.2672	0.2406	0.1746
v_2^F	0.6661	0.7594	0.9365
m_2^F	−0.0671	−0.0911	−0.1466

$$v_j^F = a^{-j}\mathcal{F}^{-1}\int_{-a}^{a} x_2^j V_1^F(0, x_2)\,\mathrm{d}x_2, \tag{6.6}$$

$$m_j^F = a^{-1-j}\mathcal{F}^{-1}\int_{-a}^{a} x_2^j M_{11}^F(0, x_2)\,\mathrm{d}x_2, \tag{6.7}$$

where the suffixes T, B, F refer to the torsion, bending and flexure problems respectively; these quantities are dimensionless and depend only upon ν. They are readily calculated once $V_1(0, x_2), M_{11}(0, x_2)$ have been found, and some of their values are listed in Table I. The necessary quadratures were performed in a similar manner to that described for the numerical evaluation of the right hand side of (4.1). As might be expected, these integrated quantities are found more accurately (for a given value of N) than are the values of the corresponding integrands; with $N = 20$, they are found correct to about 6 decimal places.

There is a valuable check which can be made on our solutions for the bending and flexure problems. By applying the reciprocity formula (C.11) to this pair of solutions, it is readily established that the constants m_2^B and v_2^F must be related by the identity

$$m_2^B + v_2^F = \frac{2(1+3\nu)}{3(1+\nu)}. \tag{6.8}$$

This identity was not used in the *calculation* of either solution but was found to be satisfied by our numerical values for m_2^B, v_2^F correct to 6 decimal places.

Additional Deflection of the Plate as $x_1 \to \infty$

As $x_1 \to \infty$, the deflection of the plate in each problem approaches that of the corresponding Saint-Venant state, except for an additional rigid body deflection. This rigid body deflection, which represents the sole effect of the clamped end condition when x_1/a is large, cannot be found independently and must be determined along

with the rest of the solution. To be precise, the deflection functions w^T, w^B, w^F in the torsion, bending and flexure problems have the form

$$w^T(x_1, x_2) = \frac{\mathcal{T}}{4D(1-\nu)}\left[\frac{x_1 x_2}{a} + \Theta^T x_2\right], \tag{6.9}$$

$$w^B(x_1, x_2) = \frac{\mathcal{M}}{4D(1-\nu^2)}\left[\frac{\nu x_2^2 - x_1^2}{a} + \Theta^B x_1 + aW^B\right], \tag{6.10}$$

$$w^F(x_1, x_2) = \frac{\mathcal{F}a}{12D(1-\nu^2)}\left[\frac{3\nu x_1 x_2^2 - x_1^3}{a^2} + \Theta^F x_1 + aW^F\right] \tag{6.11}$$

with exponentially small error as $x_1 \to \infty$. The additional rigid body deflections are associated with the dimensionless constants $\Theta^T, \Theta^B, W^B, \Theta^F, W^F$, which depend only upon ν. By further use of the reciprocal formula (C.11), these constants may be expressed in terms of the weighted integrals in Table I as follows:

$$\Theta^T = m_1^T, \tag{6.12}$$

$$\Theta^B = \nu v_2^B, \qquad W^B = -\nu v_2^F, \tag{6.13}$$

$$\Theta^F = -3\nu m_2^B, \qquad W^F = 3\nu m_2^F. \tag{6.14}$$

7. Plate of Finite Length

Although the results of previous sections apply to the semi-infinite plate, one may also treat a finite plate by regarding each of its ends as the end of an appropriate semi-infinite plate. This procedure is not exact, since the fields generated from the two ends will 'interfere' with each other. However, by examining the PF-eigenvalues in Appendix C, one may estimate the size of the error induced by neglecting this effect. The conclusion is that, for a plate* of length $2L$ and width $2a$, the relative error induced is about $(0.075)^{L/a}$ in symmetric problems and about $(0.016)^{L/a}$ in anti-symmetric problems. Thus, even for an aspect ratio as small as 2, the induced error is quite small, being about 0.6% or 0.03% respectively. Subject to this approximation, we now solve three basic problems for the rectangular plate with free sides and clamped ends.

Torsion of a Rectangular Plate with Clamped Ends

Let the plate occupy the region $|x_1| \leqslant L, |x_2| \leqslant a, |x_3| \leqslant h$ and suppose that its ends at $x_1 = \pm L$ are held in rigid clamps. Now suppose that these clamps are

* The PF-eigenvalues depend upon Poisson's ratio ν. The figures given refer to $\nu = 1/3$.

rotated through angles $\pm\alpha$ respectively about the x_1-axis so that the plate is under torsion. What resultant twisting moments $\pm\mathcal{T}$ must be applied by the clamps?

Because of the symmetry of the loading, the interior deflection function $w^I(x_1, x_2)$ (which excludes contributions decaying exponentially from each end) must have the form

$$w^I = \frac{\mathcal{T}}{4D(1-\nu)a} x_1 x_2. \tag{7.1}$$

It follows that w^+, the contribution to w that decays away from the end at $x_1 = -L$, must take the boundary values

$$w^+(-L, x_2) = -\frac{\mathcal{T}}{4D(1-\nu)} \left(\frac{L}{a}\right) x_2 + \alpha x_2, \tag{7.2}$$

$$w^+_{,1}(-L, x_2) = \frac{\mathcal{T}}{4D(1-\nu)} \left(\frac{x_2}{a}\right). \tag{7.3}$$

Now this boundary data will generate an exponentially decaying state only if it satisfies the condition (see Section 3)

$$\int_{-a}^{a} \{V_1(0, x_2) w^+(-L, x_2) - M_{11}(0, x_2) w^+_{,1}(-L, x_2)\} \, \mathrm{d}x_2 = 0, \tag{7.4}$$

where V_1, M_{11} refer to the torsion problem for the *semi-infinite* plate with (say) unit twisting moment. On substituting (7.2), (7.3) into (7.4) we find that the twist α and the twisting moment $\mathcal{T}$ must be related by

$$\alpha = \frac{\mathcal{T}}{4D(1-\nu)} \left(\frac{L}{a} + m_1^T\right). \tag{7.5}$$

Since we find that $m_1^T < 0$, the plate behaves as if it were shortened by an amount $2a(-m_1^T)$, that is, by about half a width. When $L/a = 2$, this represents a correction of about 25%.

Bending of a Rectangular plate with Clamped Ends

Suppose now that the clamps are rotated through angles $\pm\alpha$ respectively about axes parallel to the x_2-axis so that the plate is under pure bending. What resultant bending moments $\pm\mathcal{M}$ must be applied by the clamps?

In this case the symmetry of the loading means that the interior deflection function must have the form

$$w^I = \frac{\mathcal{M}}{4D(1-\nu^2)a} (\nu x_2^2 - x_1^2) + d, \tag{7.6}$$

where d is a constant yet to be determined. The boundary values of w^+ are

$$w^+(-L, x_2) = \frac{\mathcal{M}}{4D(1-\nu^2)a}(\nu x_2^2 - L^2) + d, \tag{7.7}$$

$$w^+_{,1}(-L, x_2) = \frac{\mathcal{M}}{4D(1-\nu^2)a}(2L) - \alpha. \tag{7.8}$$

These boundary values must satisfy (7.4), where V_1, M_{11} now refer to either the bending or flexure problem for the semi-infinite plate. This yields two equations for the two unknowns $\mathcal{M}, d$, from which we find that $\alpha, \mathcal{M}$ are related by

$$\alpha = \frac{\mathcal{M}}{4D(1-\nu^2)}\left[2\left(\frac{L}{a}\right) - \nu v_2^B\right]. \tag{7.9}$$

The plate thus behaves as if it were shortened by an amount $2a\nu v_2^B$.

Flexure of a Rectangular Plate with Clamped Ends

Suppose now that the clamps suffer displacements of $\pm\delta$ respectively in the x_3-direction so that the plate is under flexure. What resultant transverse forces $\pm\mathcal{F}$ must be applied by the clamps?

The solution is similar to that in the bending case and leads to the relationship

$$\delta = \frac{\mathcal{F}L^3}{12D(1-\nu^2)a}\left[2 - 3\nu v_2^B\left(\frac{a}{L}\right) + 3\nu(v_2^F - m_2^B)\left(\frac{a}{L}\right)^2 + 3\nu m_2^F\left(\frac{a}{L}\right)^3\right]. \tag{7.10}$$

Appendix A. Classical Thin Plate Theory

Suppose a plate occupies the region $\{(x_1, x_2, x_3) : (x_1, x_2) \in \mathcal{A}, |x_3| \leqslant h\}$. Then the *shear resultants* Q_α and *moment resultants* $M_{\alpha\beta}$ $(1 \leqslant \alpha, \beta \leqslant 2)$ are related to the three-dimensional stress field $\boldsymbol{\tau}(x_1, x_2, x_3)$ by

$$Q_\alpha(x_1, x_2) = \int_{-h}^{h} \tau_{\alpha 3}(x_1, x_2, x_3)\, \mathrm{d}x_3, \tag{A.1}$$

$$M_{\alpha\beta}(x_1, x_2) = \int_{-h}^{h} x_3 \tau_{\alpha\beta}(x_1, x_2, x_3)\, \mathrm{d}x_3. \tag{A.2}$$

In the classical theory of the small transverse deflection of homogeneous, isotropic, thin plates, free from body forces and surface loadings, these shear

and moment resultants are related to the transverse deflection $w(x_1, x_2)$ of the mid-plane $x_3 = 0$ by

$$Q_\alpha = -D\nabla^2 w_{,\alpha}, \tag{A.3}$$

$$M_{11} = -D(w_{,11} + \nu w_{,22}), \tag{A.4}$$

$$M_{22} = -D(w_{,22} + \nu w_{,11}), \tag{A.5}$$

$$M_{12} = -D(1-\nu)w_{,12}, \tag{A.6}$$

where w satisfies

$$\nabla^2\nabla^2 w = 0 \tag{A.7}$$

for $(x_1, x_2) \in \mathcal{A}$. In these formulae, D is the flexural rigidity of the plate, given by

$$D = \frac{2Eh^3}{3(1-\nu^2)}, \tag{A.8}$$

where E is Young's modulus and ν is Poisson's ratio for the plate.

The *effective shear resultants* V_α are defined by

$$V_1 = Q_1 + M_{12,2}, \tag{A.9}$$

$$V_2 = Q_2 + M_{21,1}. \tag{A.10}$$

If the plate has a free edge lying in $x_2 =$ constant, then the boundary conditions satisfied by the thin plate solution at this edge are Kirchhoff's contracted conditions, namely,

$$V_2 = 0, \tag{A.11}$$

$$M_{22} = 0. \tag{A.12}$$

In terms of w, these conditions take the form

$$(w_{,22} + (2-\nu)w_{,11})_{,2} = 0, \tag{A.13}$$

$$w_{,22} + \nu w_{,11} = 0. \tag{A.14}$$

Appendix B. The Corner Singularities

The form of the local eigenfunction expansions near the corners $(0, \pm a)$ has been found by Williams [7]. The individual eigenfunctions have the form

$$w = r^{\gamma+3} f(\theta), \tag{B.1}$$

Table II. Values of α, β, correct to 4 decimal places, for various ν.

ν	α	β
0	−0.6477	0
1/4	−0.9201	0.3951
1/3	−0.9380	0.4663
1/2	−0.9649	0.6020

where r, θ are plane polar co-ordinates centered at $(0, a)$ say. The governing equation (A.7) and the boundary conditions (2.1)–(2.4) imply that γ must satisfy the eigenvalue equation

$$(1-\nu)(3+\nu)\cos\pi\gamma - 2(1-\nu)^2(\gamma+2)^2 + (5+2\nu+\nu^2) = 0. \tag{B.2}$$

The general expansion near $(0, a)$ is a (complex) linear combination of eigenfunctions corresponding to those eigenvalues γ that satisfy the admissibility condition $\Re(\gamma) > -2$; this condition ensures that the corresponding strain energies are finite. Admissible eigenvalues of least real part are called *leading eigenvalues*; the corresponding *leading eigenfunctions* dominate the behaviour of w in the limit $r \to 0$.

For very small values of ν (less than about 0.035) the leading eigenvalue is real and unique. However, for all 'practical' values of ν, there is a *conjugate complex pair* of leading eigenvalues. The leading eigenvalue lying in the upper half-plane will be denoted by

$$\gamma = \alpha + i\beta. \tag{B.3}$$

Values of α, β for various ν are given in Table II. (The case $\nu = 0$ is exceptional since the 'leading' eigenvalue is $\gamma = -1$, which gives regular behaviour and so is disregarded.)

The values of $V_1(0, x_2), M_{11}(0, x_2)$ corresponding to the eigenvalue (B.3) have the form

$$V_1(0, a-r) = K_1 r^{\alpha+i\beta}, \tag{B.4}$$

$$M_{11}(0, a-r) = K_2 r^{1+\alpha+i\beta}, \tag{B.5}$$

where the ratio K_1/K_2, which depends only on ν, is given by

$$\frac{K_1}{K_2} = \frac{(\gamma+1)\{2-(1-\nu)(\gamma+3)\}}{2-(1-\nu)(\gamma+2)} \tan\frac{\pi\gamma}{2}, \tag{B.6}$$

where $\gamma = \alpha + i\beta$.

Although admissibility only requires that $\alpha > -2$, we note that, in fact, $\alpha > -1$ for $\nu > 0$. In this case then $V_1(0, x_2)$ has integrable singularities at $x_2 = \pm a$, while $M_{11}(0, x_2)$ is continuous on $[-a, a]$.

Appendix C. A Reciprocity Formula for Classical Thin Plate Theory

Let R be a domain of the (x_1, x_2)-plane enclosed by the simple closed curve* C and suppose that the deflection functions $w^{(1)}(x_1, x_2), w^{(2)}(x_1, x_2)$ satisfy the governing equation of thin plate theory (for zero loads), namely,

$$\nabla^2 \nabla w = 0, \tag{C.1}$$

$(x_1, x_2) \in R$. Then, by applying the divergence theorem, we have

$$\begin{aligned}
&\int_C \{Q_\alpha^{(1)} w^{(2)} - M_{\alpha\beta}^{(1)} w_{,\beta}^{(2)}\} n_\alpha \, \mathrm{d}t \\
&\quad = \int\int_R \frac{\partial}{\partial x_\alpha} \{Q_\alpha^{(1)} w^{(2)} - M_{\alpha\beta}^{(1)} w_{,\beta}^{(2)}\} \, \mathrm{d}x_1 \, \mathrm{d}x_2 \\
&\quad = \int\int_R \{Q_{\alpha,\alpha}^{(1)} w^{(2)} + Q_\alpha^{(2)} w_{,\alpha}^{(2)} - M_{\alpha\beta,\alpha}^{(1)} w_{,\beta}^{(2)} - M_{\alpha\beta}^{(1)} w_{,\alpha\beta}^{(2)}\} \, \mathrm{d}x_1 \, \mathrm{d}x_2 .
\end{aligned} \tag{C.2}$$

Here, summation is assumed for $1 \leqslant \alpha, \beta \leqslant 2$, the variable t measures distance around C in the anti-clockwise direction, and $\mathbf{n}(t)$ is the outward unit normal to R. Now, for zero loads, we have

$$Q_{\alpha,\alpha}^{(1)} = 0, \tag{C.3}$$

$$M_{\alpha\beta,\alpha}^{(1)} = Q_\beta^{(1)}, \tag{C.4}$$

so that the right side of (C.2) becomes

$$\begin{aligned}
&- \int\int_R M_{\alpha\beta}^{(1)} w_{,\alpha\beta}^{(2)} \, \mathrm{d}x_1 \, \mathrm{d}x_2 \\
&\quad = - \int\int_R M_{\alpha\beta}^{(2)} w_{,\alpha\beta}^{(1)} \, \mathrm{d}x_1 \, \mathrm{d}x_2
\end{aligned} \tag{C.5}$$

after using the 'stress-strain' relations (A.4)–(A.6). Hence, under the conditions assumed above, we have the reciprocity formula

$$\int_C \{Q_\alpha^{(1)} w^{(2)} - M_{\alpha\beta}^{(1)} w_{,\beta}^{(2)}\} n_\alpha \, \mathrm{d}t = \int_C \{Q_\alpha^{(2)} w^{(1)} - M_{\alpha\beta}^{(2)} w_{,\beta}^{(1)}\} n_\alpha \, \mathrm{d}t. \tag{C.6}$$

* C is also supposed to be piecewise continuously differentiable.

For our purposes, we need a formula involving V_α rather than Q_α. Let $\mathbf{t}(t)$ be the unit vector perpendicular to $\mathbf{n}(t)$ and pointing in the direction of increasing t. Then the left side of (C.6) can be written

$$\int_C \{Q_n^{(1)} w^{(2)} - M_{nn}^{(1)} w_{,n}^{(2)} - M_{nt}^{(1)} w_{,t}^{(2)}\} \, \mathrm{d}t, \tag{C.7}$$

where the suffixes n, t relate to the directions of $\mathbf{n}$, $\mathbf{t}$. If C_{AB} is any section of C *not* containing a corner, then an integration by parts shows that

$$\int_{C_{AB}} M_{nt}^{(1)} w_{,t}^{(2)} \, \mathrm{d}t = \left[M_{nt}^{(1)} w^{(2)}\right]_A^B - \int_{C_{AB}} M_{nt,t}^{(1)} w^{(2)} \, \mathrm{d}t. \tag{C.8}$$

Thus (C.7) may be written as

$$\int_C \left\{\left(Q_n^{(1)} + M_{nt,t}^{(1)}\right) w^{(2)} - M_{nn}^{(1)} w_{,n}^{(2)}\right\} \mathrm{d}t + \sum \left[\Delta M_{nt}^{(1)} w^{(2)}\right], \tag{C.9}$$

where $[\Delta M_{nt}^{(1)} w^{(2)}]$ means the jump* in the value of $M_{nt}^{(1)} w^{(2)}$ at a corner point of C (in the direction of increasing t), and the summation is over all such corner points. If we now define

$$V_n = Q_n + M_{nt,t}, \tag{C.10}$$

then (C.6), (C.9) yield the alternative reciprocity formula

$$\int_C \left\{V_n^{(1)} w^{(2)} - M_{nn}^{(1)} w_{,n}^{(2)}\right\} \mathrm{d}t + \sum \left[\Delta M_{nt}^{(1)} w^{(2)}\right]$$

$$= \int_C \left\{V_n^{(2)} w^{(1)} - M_{nn}^{(2)} w_{,n}^{(1)}\right\} \mathrm{d}t + \sum \left[\Delta M_{nt}^{(2)} w^{(1)}\right]. \tag{C.11}$$

This is the form of reciprocity used in Section 3.

Appendix D. The PF-eigenfunctions

The PF-eigenfunctions for the plate (of width 2) are solutions of the governing equation (A.7) that have the form

$$w(x_1, x_2) = g(x_2)\, \mathrm{e}^{-\lambda x_1} \tag{D.1}$$

and satisfy the Kirchhoff boundary conditions (A.13)–(A.14)on $x_2 = \pm 1$. The designation PF indicates that these eigenfunctions are analogous to the well-known Papkovich–Fadle eigenfunctions of plane strain theory.

* This jump occurs because of the jumps in $\mathbf{n}$, $\mathbf{t}$ at corner points of C.

The *symmetric eigenfunctions* (appropriate for the bending and flexure problems) have the form

$$w^{\lambda}(x_1, x_2) = E^{\lambda}(x_2)\, \mathrm{e}^{-\lambda x_1}, \tag{D.2}$$

where λ is a root of

$$\sin 2\lambda = \left(\frac{1-\nu}{3+\nu}\right) 2\lambda \tag{D.3}$$

and

$$E^{\lambda}(x_2) = \left(\lambda \cot \lambda - \frac{1+\nu}{1-\nu}\right) \cos \lambda x_2 + \lambda x_2 \sin \lambda x_2. \tag{D.4}$$

The *anti-symmetric eigenfunctions* (appropriate for the torsion problem) have the form

$$w^{\lambda}(x_1, x_2) = F^{\lambda}(x_2)\, \mathrm{e}^{-\lambda x_1}, \tag{D.5}$$

where λ is a root of

$$\sin 2\lambda = -\left(\frac{1-\nu}{3+\nu}\right) 2\lambda \tag{D.6}$$

and

$$F^{\lambda}(x_2) = \left(\lambda \tan \lambda + \frac{1+\nu}{1-\nu}\right) \sin \lambda x_2 + \lambda x_2 \cos \lambda x_2. \tag{D.7}$$

In the method of projection, we are only concerned with those eigenvalues that satisfy $\Re(\lambda) > 0$; the corresponding eigenfunctions *decay* exponentially as $x_1 \to +\infty$.

References

1. F. Erdogan, G.D. Gupta and T.S. Cooke, The numerical solutions of singular integral equations. In G.C. Sih (ed.), *Methods of Analysis and Solutions to Crack Problems*. Chapter 7, Noordhoff, Groningen (1972), pp. 368–425.
2. R.D. Gregory and I. Gladwell, The cantilever beam under tension, bending or flexure at infinity. *J. Elasticity* **12** (1982) 317–343.
3. R.D. Gregory and I. Gladwell, The reflection of a symmetric Rayleigh-Lamb wave at the fixed or free edge of a plate. *J. Elasticity* **13** (1983) 185–206.
4. W.T. Koiter and J.B. Alblas, On the bending of cantilever rectangulars plates, Parts I-IV *Proc. Kon. Nederl. Acad. Wetensch.* **B57** (1954) 250–258, 259–269, 549–557; **B60** (1957) 173–181.
5. NAG Library Manual, Mark 15, Numerical Algorithms Group Limited, Oxford, 1991.
6. S. Timoshenko and S. Woinowsky–Kreiger, *Theory of Plates and Shells*, 2nd ed. McGraw-Hill, New York, 1959.
7. M.L. Williams, Surface stress singularities resulting from various boundary conditions in angular corners of plates under bending. *U.S. National Congress of Applied Mechanics*, Illinois Institute of Technology, Chicago, Ill. (1951) 325–329.